Electrospun Silk Fibroin Nanofibers with Improved Surface Texture

Leila Salmani and Mahdi Nouri

***Abstract*— A new method for preparing silk fibroin (SF) nanofibers with an improved texture and a porous surface is proposed. In order to prepare such nanofibers, SF/Poly (ethylene glycol) (PEG) blend nanofibers were electrospun and then PEG was extracted via selective dissolution technique using methanol. The morphological structure of the electrospun nanofibers were characterized using field-emission scanning electron microscope (FE-SEM), infrared spectroscopy (FTIR, ATR), transmission electron microscopy (TEM), differential scanning calorimetry (DSC), and atomic force microscopy (AFM). Mechanical properties of the nanofiber mats were evaluated with the aid of stress-strain curves. FE-SEM and AFM images revealed a smooth surface for electrospun SF and SF/PEG blend nanofibers with an average fiber diameter in the range of 100-180 nm, while PEG extracted nanofibers showed a rough and porous surface with an average diameter in the range of 100-150 nm. The analysis of the ATR, DSC, and TEM tests revealed that SF/PEG blend is an immiscible two phase system in which PEG accumulated on the surface of the electrospun blend nanofibers. PEG extracted nanofibers showed no internal cavities with a remarkable increase in the surface roughness in comparison to SF and SF/PEG blend nanofibers.**

***Keywords*: characterization, electrospinning, poly (ethylene glycol), silk fibroin, surface roughening**

I. Introduction

Recently, many researchers in fiber and biomedical fields have got interested in fibrous protein based biopolymers, such as silk and collagen due to their unique biocompatible properties [1-3]. Silks are generally defined as fibrous proteins that are spun into fibers by some Lepidoptera larvaes such as silkworms, spiders, scorpions, mites, and flies [1,4]. Among the native silk proteins, the silkworm silk, mostly that of the domesticated Bombyx mori (B.mori) fibers, has been accepted as a high quality textile fiber and suture for a long time. B.mori silk fiber has been shown to be composed of two protein monofilaments (named fibroin) embedded in glue like sericin coating. Silk has excellent properties such as low weight (1.3 g cm^{-3}) and high tensile strength (up to 4.8 GPa as the strongest fiber known in nature) [1,5]. Silk is thermally stable up to 250˚C, allowing processing over a wide range of temperatures. In addition to the outstanding mechanical properties, silk fibroin (SF) displays good biological compatibility while the sericin glue-like proteins are not biocompatible [1,6]. In practice, SF has been used in various fields, such as cosmetics, medical materials for human health, and food additives.

Recently, several studies have been reported on the preparation of porous silk fibroin mats via different methods, such as salt leaching, freeze drying and foaming, thermal degradation, photocrosslinking, and selective dissolution [7,8].

The electrospinning process is an effective method for manufacturing ultrafine fibrous structures of many polymers with diameters in the range of several micrometers down to a few nanometers. This method seems to be the most straightforward way which produces nanofibers by forcing a polymer melt or solution through a spinneret using a high voltage electrostatic field. Several authors have explained the process; for the sake of brevity a few are mentioned in the list of references [1, 9-12].

A number of researchers have investigated silk-based electrospun nanofibers as one of the candidate materials for biomedical applications [1,13-15]. Several researchers have also studied processing parameters and morphology of electrospun silk nanofibers [1,16-20] using Hexafluoroacetone, Hexafluoro-2-propanol and formic acid as solvents for SF. In all of these reports nonporous nanofibers with a smooth surface have been observed.

Since successful application of many nanofibrous mats is related to their surface morphology, fabrication of surface porous structures is important. The surface porous structure of nanofibers in the mats plays an essential role in enhancing the performance of the nanofibrous based materials for biomedical applications. This kind of mat is important in tissue engineering. They support a place for attachment and increase the surface area, support a large cell mass, and are able to form specific structures [21].

Poly(ethylene glycol) (PEG) is a linear neutral and water soluble amphilipatic polyether [22]. PEG exhibits useful properties such as nontoxicity [22,23], non-antigenic [24], biocompability and high water solubility [23,25]. PEG is soluble in organic solvents such as methylene chloride, ethanol, methanol, acetone and chloroform [22].

In this study, silk fibroin (SF) nanofibers with a rough and porous surface were fabricated via electrospinning followed by selective dissolution technique. A solution of SF/PEG blend in formic acid was electrospun and PEG was selectively extracted using methanol as a solvent for PEG.

L. Salmani and M. Nouri are with the Department of Textile Engineering, Faculty of Engineering, University of Guilan, Rasht, Iran. Correspondence should be addressed to M. Nouri (e-mail: mnouri69@guilan.ac.ir).

II. Materials and Methods

A. Preparation of Regenerated Silk Fibroin (SF) Solution

Silks were obtained from a domestic producer, Abrisham Guilan, Iran. The chemicals, Na_2CO_3, C_2H_5OH and formic acid were from Merck, Germany, and used as received. The silks were treated three times with a 0.05 wt % Na_2CO_3 solution at 100°C for 30 min to remove sericin, and then were rinsed and air dried. The pure silk fibroin fibers were dissolved in a ternary solvent $CaCl_2$ /CH_3CH_2OH/ H_2O (mole ratio 1:2:8) at 78 ± 2°C for 2 h through stirring. The prepared solution was dialyzed against distilled water for three days using a cellulose tubular membrane (Dialysis Tubing D9527, Sigma) and then lyophilized to form regenerated SF sponges. Regenerated silk fibroin and PEG were dissolved in 98% formic acid for 30 min to prepare 10% (W/V) solutions with SF/PEG blend ratios of 100/0, 90/10, 80/20, 70/30, 60/40, and 50/50.

B. Electrospinning

In the electrospinning process, a high electric potential (Gamma High voltage Research) was applied to a droplet of SF solution at the tip of a syringe needle (0.35 mm inner diameter). The electrospun nanofibers were collected on a target plate (aluminum foil), which was placed at a distance of 10 cm from the syringe tip. A syringe pump (New Eva Pump System) was used to form a constant amount of SF solution at the syringe tip. The output of the injection pump was 0.2 μL min^{-1} at 25°C. A charged jet is formed and ejected in the direction of the applied field. The applied electrical potential was 9 kV. As the SF/PEG solution jet travels in the air, most of the solvent evaporates and the SF/PEG blend is collected on the grounded target in a fine fibrous form. The syringe tip and the target plate were enclosed in a chamber for adjusting and controlling the temperature. After spinning, the prepared SF/PEG nanofibrous web was removed from foil and immersed in methanol (99%) for 24 h to remove PEG from the nanofibers.

C. Characterization

Morphology and dimension of the gold-sputtered electrospun nanofibers were determined using a FE-SEM S4160 scanning electron microscopy, Hitachi, Japan. Measurements of about 50 random points on the fibers were used for determining fiber diameter distribution and the average fiber diameter. The surface texture of nanofibers was studied by Atomic Force microscopy (AFM) Nanowizard II, JPK CO., Germany. A high-resolution transmission electron microscopy (TEM, Zeiss-EM10C-80 kV) was also employed to observe the morphological structures of the PEG extracted SF nanofibers. FTIR-ATR spectra of the as_spun and solvent treated samples were recorded with a FTIR-ATR Nicolet Magna_IR 560 spectrometer (USA) in the spectra region of 4000–400 cm^{-1}. Density of the samples was measured by the flotation method at 20 ± 0.05°C.

Thermal characteristics of the mats were recorded with the aid of BAHR Thermo analyse DSC 302 differential scanning calorimeter. About 4 mg the sample was heated at a heating rate of 5 ^oC min^{-1} under a constant nitrogen flow.

Mechanical properties of the as-spun and solvent treated mats were determined using Shirley micro50 fiber tensile tester. Samples of mats with known area density were cut into strips with dimensions of 2 × 0.5 cm and then were mounted at the tensile tester grips. The strain rate and gage

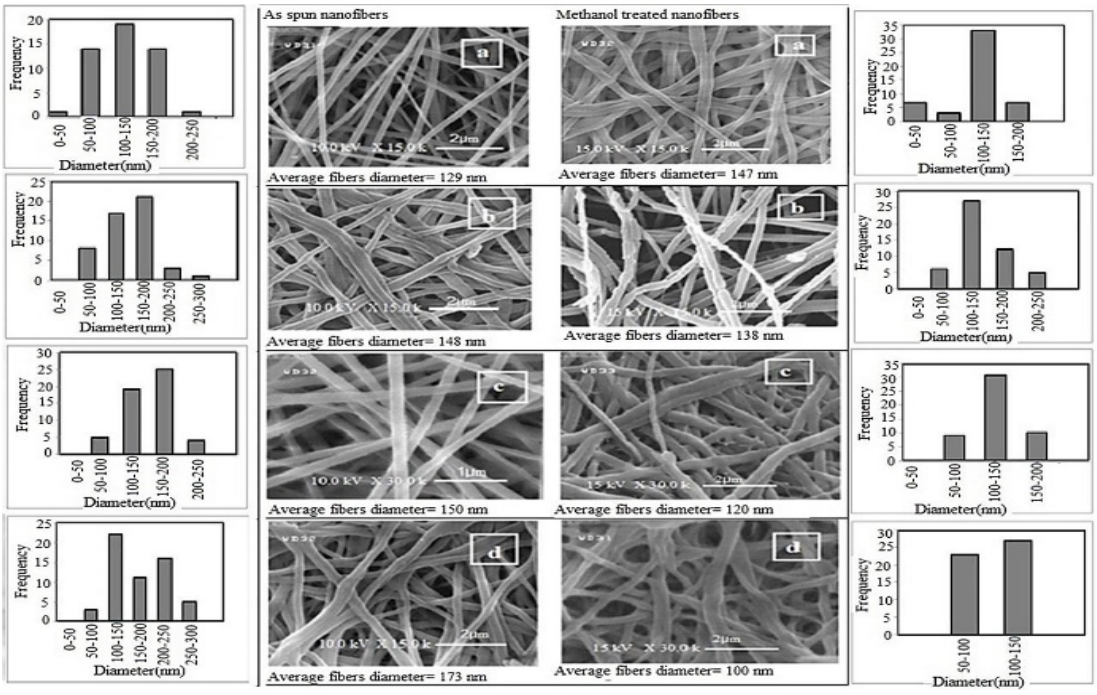

Fig. 1. FE-SEM images of SF/PEG fibers before and after methanol treatment, with SF/PEG ratio of: (a) 100/0, (b) 90/10, (c) 80/20, and (d) 70/30.

length in the measurements were 1 mm min^{-1} and 1 cm, respectively. At least 3 samples were tested and their stress-strain curves were recorded. The results of the tensile strength and strain were averaged and reported.

III. Results and Discussion

A. FE-SEM of Electrospun Fibers

To study the effect of PEG content on the morphology and texture of SF/PEG electrospun nanofibers, all the electrospinning processing variables were kept constant. Nanofibers were produced using SF and SF/PEG blends with a PEG content that ranged between 10 and 50 wt%. Electrospinning were performed at 9 kV, while the solution concentration was equal to 10 wt%. FE-SEM images and diameter distribution of the SF and SF/PEG electrospun fibers are shown in Fig. 1. As shown in this figure, the electrospinning of blend solutions resulted in circular structures. It was found that increasing PEG content at constant process parameters increases the average fiber diameter significantly. For instance, the average fiber diameter at SF/PEG weight ratio of 90/10 was 148 nm, while at a weight ratio of 70/30 the average fiber diameter was 173 nm. Attempts to obtain fibrous structures from the SF/PEG blend solutions with a higher content of PEG were unsuccessful and too many beads instead of nanofibers were formed. This could be attributed to the low viscosity of these blend solutions, which hinders the formation of a stable drop at the tip of the needle. Generally, there is a critical viscosity for an electrospinable solution; below this viscosity, chain entanglements would be insufficient to stabilize the coulombic repulsion within the ejected jet, leading to the formation of sprayed droplets.

Fig. 1 shows the FE-SEM images and fiber diameter of the PEG extracted fibers. This figure shows an irregular and rough nanofiber surface after extraction of PEG from SF/PEG electrospun nanofibers. This surface irregularity and roughness may be due to removing of PEG from the surface of SF/PEG nanofibers.

TABLE I
Density and Weight Loss of SF and SF/PEG Blend Nanofibers Before and After Extraction of PEG

SF/PEG blend ratio	Weight% of PEG	Density of samples (g cm^{-3})		Weight % of extracted PEG	Fiber Diameter	
		Before extraction of PEG	After extraction of PEG		Before extraction of PEG	After extraction of PEG
100/0(SF)	0	1.5672 ± 0.0025	1.5672 ± 0.0025	---	129.26	147
90/10	10	1.4094 ± 0.0035	1.5661± 0.0012	11.9	148.437	138.1
80/20	20	1.3873± 0.0037	1.5669 ± 0.0015	18.9	150.737	120.036
70/30	30	1.3513± 0.0022	1.5671 ± 0.0027	27.3	173.18	100.569

Table I summarizes the average fiber diameters of as-spun SF/PEG and methanol treated SF/PEG (PEG extracted) electrospun fibers. The results indicate that the averages of fibers diameter decreased after extraction of PEG from SF/PEG electrospun fibers which reveal the removing of PEG from the surface of the nanofibers. Table I also shows that the average fiber diameters decreased from 148 nm to 138 nm for 90/10 SF/PEG sample, and from 173 nm to 100 nm for 70/30 SF/PEG sample. These results reveal that with increasing the PEG content in SF/PEG blends more decrease in the average fiber diameter is observed which may be due to more accumulation of PEG on the surface of high PEG content SF/PEG electrospun nanofibers.

B. FTIR-ATR Spectroscopy

FTIR spectroscopy is a suitable method for studying the conformational changes of the secondary structure of silk fibroin [26]. Fig. 2(B) shows the FTIR spectra of electrospun nanofibers before and after removing PEG, in the range of 400-4000 cm^{-1}. PEG spectrum [Fig. 2(A)] shows characteristic bands at 1106-1113 and 2874 cm^{-1}. The peak at 1106-1113 cm^{-1} is attributed to the stretching vibration of C-O functional groups and the peak at 2878 cm^{-1} represents the stretching vibration of $–CH_2$ [27]. Fig. 2(B) represents the FTIR spectra of the structure of as spun and methanol treated SF/PEG mats. According to this figure, the characteristic bands of PEG at 1113 and 2874 cm^{-1} in the SF/PEG nanofibers spectra confirms the existence of PEG at the SF/PEG blend fibers, while disappearance of these characteristic bands in the spectra of methanol treated mats confirms the complete extraction of PEG from the nanofibers during the methanol treatment.

SF exists in three conformations as: random coil, silk I (α-random coil) and silk Π(β-sheet) [26]. The peak at 1655 cm^{-1} (amid I, C=O stretching), 1540 cm^{-1} (amid Π, N-H deformation) and 1242 cm^{-1} (amid III, C-N stretching and C=O bending vibration) indicates a random coil conformation [26]. SF molecules can structurally rearrange to β-sheet conformation due to a change in the hydrogen bonding by ethanol or methanol treatment [26]. This kind of conformational rearrangement may happen by extraction of PEG from SF/PEG blend fibers during methanol treatment of blend nanofibers. As shown in Fig. 2(B), the transition from random coil to β-sheet conformation during extraction of PEG is confirmed by the shift in the characteristic bands (1629 cm^{-1}, 1524 cm^{-1} and 1235 cm^{-1}) to lower wave numbers in the spectra of methanol treated mats.

In order to calculate the degree of crystallinity of SF, the position of the amide I band was analyzed because as mentioned above, the position of the peak in the spectrum of the crystalline β-sheets is different from that of the random coil structures [19]. The intensity ratio of I_{1629}/I_{1655} can be used to define an IR crystallinity index (C.I) for SF [26]. Using FTIR spectra, the C.I of the SF and SF/PEG fibers were calculated and presented in Table II. As shown in this table, with increase in the PEG content of SF/PEG blend nanofibers, the C.I also increases, which shows the conformational change of SF molecules from random coil to β-sheet structure. This conformational change is due to

the intermolecular hydrogen bond formation between SF and PEG molecules in the blend fibers.

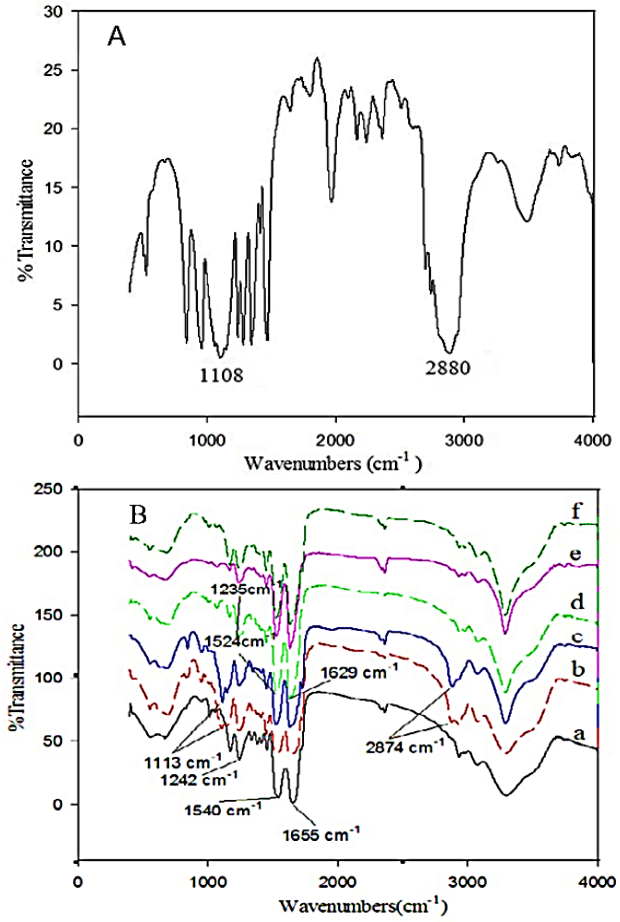

Fig. 2. FTIR Spectrum of (A) PEG; and (B) SF/PEG blend nanofibers before methanol treatment (graphs a, b and c) with SF/PEG ratio of (a) 0/100, (b) 80/20, and (c) 70/30; and after methanol treatment (graphs d, e, and f) with SF/PEG ratio of (d) 0/100, (e) 80/20, and (f) 70/30.

TABLE II
CRYSTALLINITY INDEX OF SF IN SF/PEG BLEND NANOFIBERS WITH VARIOUS BLEND RATIOS CALCULATED FROM FTIR SPECTRA

SF/PEG blend ratio	Crystallinity index (Intensity ratio of I_{1629}/I_{1655})
100/0 (SF)	0.5
90/10	0.9
80/20	1.09
70/30	1.42

ATR spectroscopy provides a method for analyzing the availability of PEG on the surface of the SF/PEG blend fibers [28]. Fig. 3 shows the ATR spectra of SF and SF/PEG blend nanofibers. Compared with the ATR spectrum of SF, the peaks at 1111 cm^{-1} and 2874 cm^{-1} on the blend nanofibers confirm the availability of PEG on the surface of the SF/PEG blend fibers. The PEG content of the samples may be evaluated by intensity ratio of I_{1113}/I_{1540} in the FTIR or ATR spectra. Table III shows the blend ratios of PEG to SF which were calculated by the I_{1113}/I_{1540} intensity obtained from ATR and FTIR spectra. By comparing the PEG content of the samples it might be said that most of the PEG molecules are distributed and accumulated on the surface of the SF/PEG blend nanofibers.

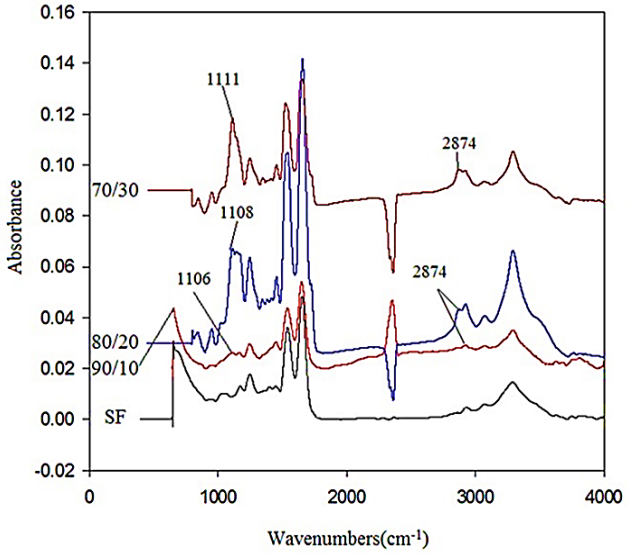

Fig. 3. ATR spectra of as spun SF and SF/PEG blend nanofibers.

TABLE III
PEG CONTENT OF SF/PEG BLEND NANOFIBERS ESTIMATED FROM FTIR AND ATR SPECTRA

Theoretical SF/PEG blend ratio	PEG content (%) estimated from ATR spectra (Intensity ratio of I_{1113}/I_{1540})	PEG content (%) estimated from FTIR spectra (Intensity ratio of I_{1113}/I_{1540})
90/10	26.16	14.91
80/20	56.34	24.65
70/30	90.62	41.42

C. Density and Weight Loss of the Electrospun Fibers

Porous fibers may be prepared by selective dissolution, thermal degradation, or photo-degradation of one component in hybrid fibers [29]. In this study, PEG was removed from the SF/PEG blend fibers via a selective dissolution method. Table I summarizes the weight loss of the remaining SF fibers after dissolution of PEG with methanol, which was determined by weighing of the dried fibers before and after dissolving PEG. The results in table I show that the weight of the mats after methanol treatment was reduced by 10%, 20% and 30% for 90/10, 80/20 and 70/30 samples, respectively. This confirms that most of the PEG molecules were extracted during methanol treatment of the mats. Table I also represents density of the as-spun SF/PEG and PEG extracted fibers. The density of the samples was measured in a Hexane/carbon tetrachloride mixture. The density of pure SF and PEG are 1.567 and 1.212 g cm^{-3}, respectively. The results in table I show an insignificant difference between the density of the SF and PEG extracted nanofibers which confirm the accumulation of PEG on the surface of the SF/PEG blend fibers.

D. AFM and TEM Analysis

AFM analysis was performed to measure the roughness value and to investigate the surface morphology of SF and SF/PEG blend nanofibers. Fig. 4 shows representative three dimensional topographic scan and line height profile of the SF, SF/PEG blend fibers and PEG extracted fibers. As shown in Fig. 4 the surface morphology of PEG extracted fibers differed from SF and SF/PEG blend nanofibers. The SF and SF/PEG blend nanofibers had a smooth surface with cylindrical structure while the PEG extracted fibers have a rougher surface. The cross-section at each AFM image was analyzed in terms of surface average roughness and the results were summarizes in Table IV. The SF and SF/PEG blend nanofibers had root-mean-square roughness (rms) of 6.028 and 8.953 nm, respectively, while the PEG extracted nanofibers had rms roughness of 21.48 nm. This reveals a remarkable change in the roughness of the fibers after treatment, and a rougher surface for the PEG extracted fibers.

TABLE IV
AFM VALUES OF SF AND SF/PEG BLEND NANOFIBERS BEFORE AND AFTER EXTRACTION OF PEG

Samples	Average roughness R_a (nm)	Peak to valley R_t (nm)	RMS (nm)
SF	4.984	28.81	6.028
SF/PEG before extraction of PEG	7.857	34.33	8.953
SF/PEG after extraction of PEG	18.56	82.56	21.48

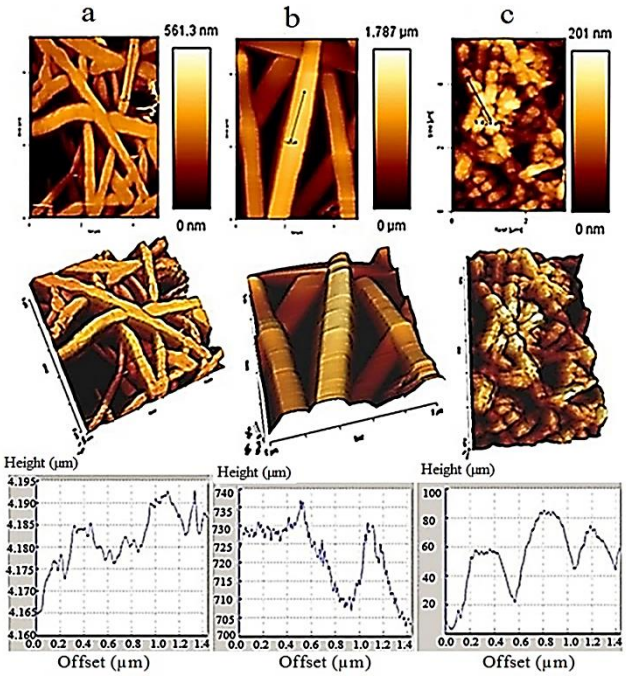

Fig. 4. AFM images and line profile of SF, SF/PEG blend nanofibers before and after methanol treatment: (a) SF, (b) 70/30 SF/PEG before methanol treatment, (c) 70/30 SF/PEG after methanol treatment.

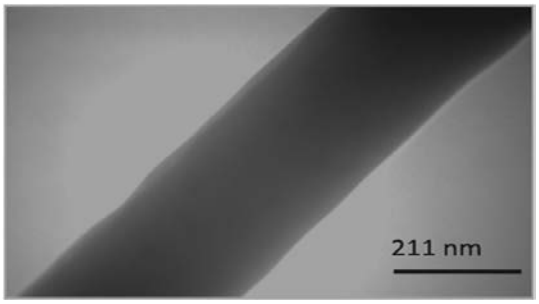

Fig. 5. TEM image of 70/30 SF/PEG nanofiber after methanol treatment.

Fig. 5 shows a representative TEM image of the PEG extracted nanofiber. As shown in this figure the fiber does not have any internal cavity. The results obtained from FE_SEM, AFM and TEM images indicate that the PEG molecules were only distributed on the surface of the SF/PEG electrospun nanofibers. In fact, the SF/PEG blend solution separates into two phase systems during electrospinning due to immiscibility of SF and PEG. An SF rich phase moves to the core of the electrospun fiber and a PEG rich phase accumulates on the surface of the fiber. During methanol treatment of this blend nanofiber, PEG is extracted from the surface which results in a nanofiber with a rough surface without any internal cavity, as shown in the AFM and TEM images.

E. Thermal Behavior of Electrospun Fibers

The interaction between SF and PEG was investigated using DSC thermograms. The DSC thermograms of SF, PEG and SF/PEG electrospun nanofibers are shown in. The DSC curve of SF, Fig. 6(a), shows two endothermic peaks at 80°C and 284°C, due to the loss of water and thermal degradation of SF chains, respectively. In this figure, the weak endothermic peak at about 170-180°C and the exothermic peak at 268°C correspond to the glass transition temperature (T_g) of SF with a random coil conformation, and conformational transition from random coil to β-sheet structure, respectively. These are in the range of the reported values for SF [30]. The thermogram curve of PEG, Fig. 6(b), shows an intense endothermic peak at 62°C which corresponds to the melting point of PEG [31].

Fig. 6(c) shows the DSC thermograms of SF/PEG blend nanofibers. These curves show an endothermic peak at 60-70°C due to the melting point of PEG and loss of water of SF. The exothermic peak at 265-270°C is due to conformational transition from random coil to β-sheet structure of SF, as seen in the DSC thermogram of pure SF fibers. Furthermore, a new exothermic peak has appeared at 181-204°C which corresponds to the conformational transition of SF molecules from random coil to β-sheet structure in the presence of PEG. This decrease in conformational transition temperature is due to plasticizing effect of flexible PEG molecules which increases the flexibility of SF chains. This result confirms once again the formation of two phase systems in the SF/PEG blend nanofibers as previously observed by FTIR and AFM results.

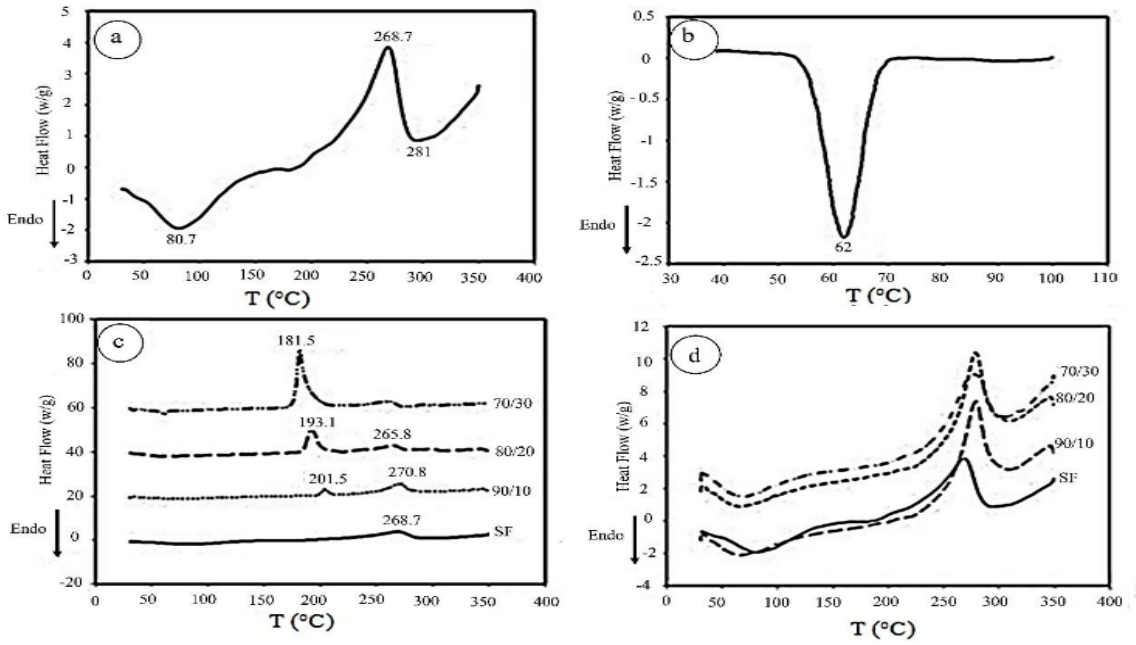

Fig. 6. DSC thermograms of nananofibers: (a) SF, (b) PEG, (c) SF/PEG fibers before methanol treatment, and (d) SF/PEG after methanol treatment.

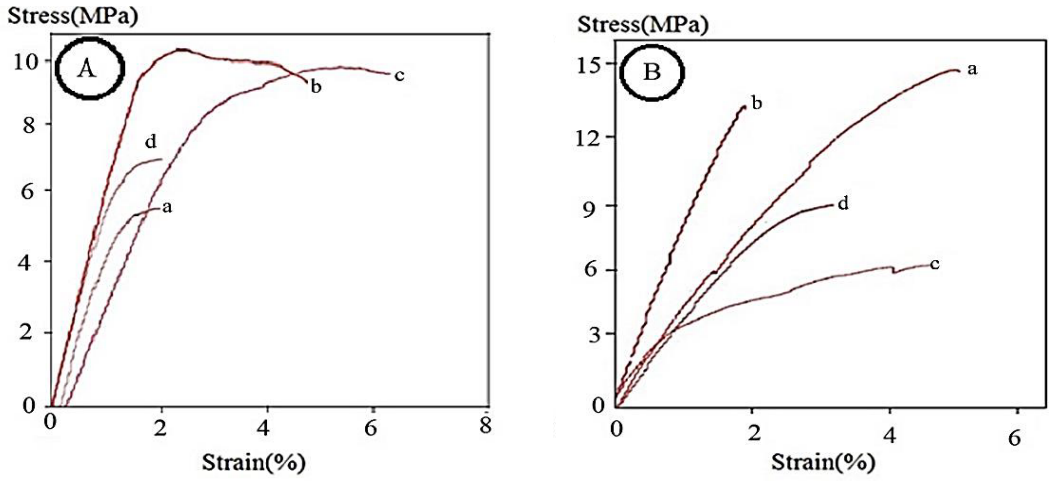

Fig. 7. Stress-strain curves of SF and SF/PEG blend nanofibrous mats. (A) Before methanol treatment with SF/PEG ratio of (a) 100/0, (b) 90/10, (c) 80/20, and (d) 70/30; and (B) after methanol treatment with SF/PEG ratio of (a) 100/0, (b) 90/10, (c) 80/20, and (d) 70/30.

Fig. 6(d) shows the DSC thermograms of methanol treated samples. In these curves the endothermic peak at 60-65°C has disap peared and a typical DSC thermogram of pure SF is observed which shows the complete extraction of PEG from the blend fibers during methanol treatment.

F. Mechanical Properties of the Mats

The mechanical properties of the electrospun fibers were recorded in stress (GPa) vs. strain (%) data. The ultimate stress was calculated by using Eq. (1):

$$S = \frac{\rho \times B}{A \times W} \quad (1)$$

where S is the stress in GPa, B is the breaking load in g, ρ is the density of nanofibers, A is the area density in $g.m^{-2}$, and W is the specimen width in m. The initial modulus of the samples was calculated from the slop of the initial part of the load strain curve.

Fig. 7 shows typical stress-strain curves of the SF mats electrospun with various blend ratios before and after extraction of PEG. The stress-strain curves of the mats demonstrate similar characteristics. The initial part of these curves shows a high resistance to deformation due to the cohesive force in the fiber assembly as a result of the large number of fiber to fiber contacts. A distinct yield point is observed after the initial part of the stress-strain curves followed by a gradual decrease in modulus caused by fiber slippage. Further increase in deformation led to the decrease in the cross section of the specimens resulting from the failure of fiber assemblies.

The mechanical properties of the samples are listed in Table V. It is evident that the pure SF nanofiber mats had a lower tensile strength in comparison to SF/PEG blends. This may be due to the lower flexibility of SF chains. The mechanical properties of the SF/PEG blend fiber mats are greatly improved with increase in the PEG content. With

addition of PEG, the structure of nanofibers becomes more elastic. PEG can diffuse into silk fibroin polymer chains due to its low molecular weight and increase the movement of silk fibroin polymer chains which results in higher strain as shown in table V. The results of mechanical properties of PEG extracted samples [Fig. 7(B), Table V] show that the tensile strength was enhanced and the strain decreased during methanol treatment. Among these samples, pure SF has a higher tensile strength which may be due to smoother surface and lesser surface defects in comparison to the PEG extracted SF nanofibers.

TABLE V
MECHANICAL PROPERTIES OF SF AND SF/PEG BLEND NANOFIBERS BEFORE AND AFTER EXTRACTION OF PEG

SF/PEG blend ratio	Before extraction of PEG		After extraction of PEG	
	Strain (%)	Stress (MPa)	Strain (%)	Stress (MPa)
100/0 (SF)	2.1	5.6	5.1	15
90/10	7.45	9.1	1.9	13.3
80/20	5.5	9.6	4.7	6.43
70/30	2.2	6.2	2.9	9.9

IV. CONCLUSION

The SF/PEG blend nanofibers, prepared by electrospinning of SF/PEG solutions in formic acid, were round in shape with an average diameter in the range of 130-180 nm. SF/PEG fibers showed a two phase system, due to immiscibility of SF and PEG, consisting of a PEG rich phase and an SF rich phase. TEM, AFM and ATR-FTIR results showed that the PEG rich phase accumulates at the surface of the SF/PEG electrospun nanofibers.

PEG was completely removed during methanol treatment, in which conformational change of SF chains from random coil to β-sheet structure occurred. TEM and AFM analysis of the remaining SF fibers showed no internal cavity and a very rough and porous surface in comparison to electrospun SF and SF/PEG blend nanofibers. SF/PEG nanofibers showed enhanced mechanical properties in comparison to pure SF due to the plasticizing effect of the PEG molecules.

REFERENCES

[1] N. Amiraliyan, M. Nouri, and M. Haghighat Kish, "Effects of some electrospinning parameters on morphology of natural silk-based nanofibers", *J. Appl. Polym. Sci.*, vol. 113, no. 1, pp. 226-234, 2009.

[2] G. H. Altman, F. Diaz, C. Jakuba, T. Calabro, R. L. Horan, J. Chen, H. Lu, J. Richmond, and D. L. Kaplan, "Silk-based biomaterials", *Biomaterials*,vol. 24, no. 3, pp. 401-416, 2003.

[3] Y. Zhang, J. Venugopal, Z. M. Huang, C. Lim, and S. Ramakrishna, "Crosslinking of the electrospun gelatin nanofibers", *Polymer*, vol. 47, no. 8, pp. 2911-2917, 2006.

[4] D. Kumar and R. R. Kundapur, *Biomedical Applications of Natural Proteins*, Bangalore: springer, 2015, pp. 51-56.

[5] Y. Wang, H. J. Kim, G. Vunjak Novakovic, and D. L. Kaplan, "Stem cell-based tissue engineering with silk biomaterials", *Biomaterials*, vol. 27, no. 36, pp. 6064-6082, 2006.

[6] I. C. Um, H. Y. Kweon, K. G. Lee, and Y. H. Park, "The role of formic acid in solution stability and crystallization of silk protein polymer", *Int. J. Biol. Macromol*., vol. 33, no. 4, pp. 203-213, 2003.

[7] J. Zhan, X. Sun, F. Cui, and X. Kong, "Preparation of 3-D porous fibroin scaffolds by freeze drying with treatment of methanol solutions", *Chinese. Sci. Bull*., vol. 52, no. 13, pp. 1791-1795, 2007.

[8] L. Jun, Y. Zhang, Y. Hao, L. Cheng, and Z. JJ, "Preparation of porous electro-spun UPM fibers via photocrosslinking", *J. Appl. Polym. Sci.*, vol. 112, no. 4, pp. 2247-2254, 2009.

[9] J. Deitzel, J. Kleinmeyer, D. Harris, and N. Beck Tan, "The effect of processing variables on the morphology of electrospun nanofibers and textiles", *Polymer*, vol. 42, no. 1, pp. 261-272, 2001.

[10] Z-M. Huang, Y-Z. Zhang, M. Kotaki, and S. Ramakrishna, "A review on polymer nanofibers by electrospinning and their applications in nanocomposites", *Compos. Sci. Technol*., vol. 63, no. 15, pp. 2223-2253, 2003.

[11] S. Theron, E. Zussman, and A. Yarin, "Experimental investigation of the governing parameters in the electrospinning of polymer solutions", *Polymer*, vol. 45, no. 6, pp. 2017-2030, 2004.

[12] S. Tan, R. Inai, M. Kotaki, and S. Ramakrishna, "Systematic parameter study for ultra-fine fiber fabrication via electrospinning process", *Polymer*, vol. 46, no. 16, pp. 6128-6134, 2005.

[13] N. Minoura, S. I. Aiba, Y. Gotoh, M. Tsukada, and Y. Imai, "Attachment and growth of cultured fibroblast cells on silk protein matrices", *J. Biomed. Mater. Res*., vol. 29, no. 10, pp. 1215-1221, 1995.

[14] H. J. Jin, J. Chen, V. Karageorgiou, G. H. Altman, and D. L. Kaplan, "Human bone marrow stromal cell responses on electrospun silk fibroin mats", *Biomaterials*, vol. 25, no. 6, pp. 1039-1047, 2004.

[15] L. Meinel, V. Karageorgiou, S. Hofmann, R. Fajardo, B. Snyder, C. Li, L. Zichner, R. Langer, G. Vunjak-Novakovic, and D. L. Kaplan, "Engineering bone-like tissue in vitro using human bone marrow stem cells and silk scaffolds", *J. Biomed. Mater .Res. Part A*., vol. 71, no. 1, pp. 25-34, 2004.

[16] Y. Kawahara, A. Nakayama, N. Matsumura, T. Yoshioka, and M. Tsuji, "Structure for electro-spun silk fibroin nanofibers", *J. Appl. Polym. Sci.*, vol. 107, no. 6, pp. 3681-3684, 2008.

[17] S. Zarkoob, R. Eby, D. H. Reneker, S. D. Hudson, D. Ertley, and W. W. Adams, "Structure and morphology of electrospun silk nanofibers", *Polymer*, vol. 45, no. 11, pp. 3973-3977, 2004.

[18] S. Sukigara, M. Gandhi, J. Ayutsede, M. Micklus, and F. Ko, "Regeneration of Bombyx mori silk by electrospinning. Part 2. Process optimization and empirical modeling using response surface methodology", *Polymer*, vol. 45, no. 11, pp. 3701-3708, 2004.

[19] J. Ayutsede, M. Gandhi, S. Sukigara, M. Micklus, H-E. Chen, and F. Ko, "Regeneration of Bombyx mori silk by electrospinning. Part 3: characterization of electrospun nonwoven mat", *Polymer*, vol. 46, no. 5, pp. 1625-1634, 2005.

[20] K. Ohgo, C. Zhao, M. Kobayashi, and T. Asakura, "Preparation of non-woven nanofibers of Bombyx mori silk, Samia cynthia ricini silk and recombinant hybrid silk with electrospinning method", *Polymer*, vol. 44, no. 3, pp. 841-846, 2003.

[21] Z. She, B. Zhang, C. Jin, Q. Feng, and Y. Xu, "Preparation and in vitro degradation of porous three-dimensional silk fibroin/chitosan scaffold", *Polym. Degrad. Stabil*., vol. 93, no. 7, pp. 1316-1322, 2008.

[22] K. D. Hinds and S. W. Kim, "Effects of PEG conjugation on insulin properties", *Adv. Drug deliver. Rev*., vol. 54, no. 4, pp. 505-530, 2002.

[23] X. Yang, Q. Zhang, Y. Wang, H. Chen, H. Zhang, F. Gao, and L. Liu, "Self-aggregated nanoparticles from methoxy poly (ethyleneglycol)-modified chitosan: Synthesis; characterization; aggregation and methotrexate release in vitro", *Colloid. Surface. B*., vol. 61, no. 2, pp. 125-131, 2008.

[24] M. Ahmed, N. Okasha, S. Mansour, and S. El-Dek, "Bi-modal improvement of the physico-chemical characteristics of PEG and MFe2O4 subnanoferrite", *J. Alloy. Compd*., vol. 496, no. 1, pp. 345-350, 2010.

[25] M. Zhang, X. Li, Y. Gong, N. Zhao, and X. Zhang, "Properties and biocompatibility of chitosan films modified by blending with PEG", *Biomaterials*, vol. 23, no. 13, pp. 2641-2648, 2002.

[26] N. Amiraliyan, M. Nouri, and M. Haghighat Kish, "Structural characterization and mechanical properties of electrospun silk fibroin nanofiber mats", *Polym. Sci. Ser. A Polym. Phys.*, vol. 52, no. 4, pp. 407-412, 2010.

[27] W. W. Yao, T. C. Bai, J. P. Sun, C. W. Zhu, J. Hu, and H. L. Zhang, "Thermodynamic properties for the system of silybin and poly (ethylene glycol) 6000", *Thermochim. Acta*., vol. 437, no. 1, pp. 17-20, 2005.

[28] S. Hofmann, C. Wong Po Foo, F. Rossetti, M. Textor, G. Vunjak Novakovic, D. Kaplan, H. Merkle, and L. Meinel, "Silk fibroin as an organic polymer for controlled drug delivery", *J. Control. Release*., vol. 111, no. 1, pp. 219-227, 2006.

[29] S. O. Han, W. K. Son, D. Cho, J. H. Youk, and W. H. Park, "Preparation of porous ultra-fine fibres via selective thermal degradation of electrospun polyetherimide/poly (3-hydroxybutyrate-hydroxyvalerate) fibres", *Polym. Degrad. Stabil.*, vol. 86, no. 2, pp. 257-262, 2004.

[30] A. Vasconcelos, A. C. Gomes, and A. Cavaco Paulo, "Novel silk fibroin/elastin wound dressings", *Acta. Biomater.*, vol. 8, no. 8, pp. 3049-3060, 2012.

[31] Y. Gotoh, M. Tsukada, T. Baba, and N. Minoura, "Physical properties and structure of poly (ethyleneglycol)-silk fibroin conjugate films", *Polymer*, vol. 38, no. 2, pp. 487-490, 1997.